Pediatr Nephrol (2009) 24:2361–2368
DOI 10.1007/s00467-009-1287-6

ORIGINAL ARTICLE

Functional analysis of *BMP4* mutations identified in pediatric CAKUT patients

Mansoureh Tabatabaeifar · Karl-Peter Schlingmann · Mieczyslaw Litwin · Sevinc Emre · Aysin Bakkaloglu · Otto Mehls · Corinne Antignac · Franz Schaefer · Stefanie Weber · ESCAPE Trial Group

Received: 29 April 2009 / Revised: 30 June 2009 / Accepted: 30 June 2009 / Published online: 14 August 2009

Abstract Human congenital anomalies of the kidney and urinary tract (CAKUT) represent the major causes of chronic renal failure (CRF) in children. This set of disorders comprises renal agenesis, hypoplasia, dysplastic or double kidneys, and/or malformations of the ureter. It has recently been shown that mutations in several genes, among them *BMP4*, are associated with hereditary renal developmental diseases. In *BMP4*, we formerly identified three missense mutations (S91C, T116S, N150K) in five pediatric CAKUT patients. These *BMP4* mutations were subsequently studied in a cellular expression system, and here we present functional data demonstrating a lower level of messenger RNA (mRNA) abundance in Bmp4

ESCAPE Network collaborators: A. Anarat (Adana); A. Bakkaloglu, F. Ozaltin (Ankara); A. Peco-Antic (Belgrade); U. Querfeld, J. Gellermann (Berlin); P. Sallay (Budapest); D. Drozdz (Cracow); K.-E. Bonzel, A.-M. Wingen (Essen); A. Zurowska, I. Balasz (Gdansk); F. Perfumo, A. Canepa (Genoa); D.E. Müller-Wiefel, K. Zepf (Hamburg); G. Offner, B. Enke (Hannover); O. Mehls, F. Schaefer, E. Wühl, C. Hadtstein (Heidelberg); U. Berg, G. Celsi (Huddinge); S. Emre, A. Sirin, I. Bilge (Istanbul); S. Çaliskan (Istanbul-Cerrahpasa); S. Mir, E. Serdaroglu (Izmir); C. Greiner, H. Eichstädt, S. Wygoda (Leipzig); K. Hohbach-Hohenfellner (Mainz); N. Jeck, G. Klaus (Marburg); A. Appiani, G. Ardissino, S. Testa (Milano); G. Montini (Padova); C. Antignac, P. Niaudet, M. Charbit (Paris); J. Dusek (Prague); A. Caldas-Afonso, A. Teixeira (Porto); S. Picca, C. Matteucci (Rome); M. Wigger (Rostock); M. Fischbach, J. Terzic (Strasbourg); J. Fydryk, T. Urasinski (Szezecin); R. Coppo, L. Peruzzi (Torino); A. Jankauskiene (Vilnius); M. Litwin, M. Abuauba, R. Grenda (Warszawa); K. Arbeiter (Vienna); T.J. Neuhaus (Zurich).

M. Tabatabaeifar · O. Mehls · F. Schaefer · S. Weber (✉)
Pediatric Nephrology,
University of Heidelberg Children's Hospital,
Im Neuenheimer Feld 430,
69120 Heidelberg, Germany
e-mail: stefanie.weber@med.uni-heidelberg.de

K.-P. Schlingmann
Pediatric Nephrology, University of Marburg Children's Hospital,
Marburg, Germany

M. Litwin
Nephrology and Kidney Transplantation Department,
Children's Memorial Health Hospital Warsaw,
Warsaw, Poland

S. Emre
Department of Pediatrics, Istanbul Medical Faculty,
University of Istanbul,
Istanbul, Turkey

A. Bakkaloglu
Faculty of Medicine, Hacettepe University,
Ankara, Turkey

C. Antignac
INSERM U574, Hôpital Necker-Enfants Malades,
Paris, France

Present Address:
S. Weber
University of Essen Children's Hospital,
Hufelandstrasse 55,
45122 Essen, Germany

mutants that indicates a possible negative feedback of the mutants on their own mRNA expression and/or stability. Furthermore, we describe the formation of alternative protein complexes induced by the S91C-*BMP4* mutation, which results in perinuclear endoplasmic reticulum (ER) accumulation and enhanced lysosomal degradation of Bmp4. This work further supports the role of mutations in *BMP4* for abnormalities of human kidney development.

Keywords Kidney development · CAKUT · Bone morphogenetic protein 4 · Abnormal protein complex · Subcellular localization

Introduction

Congenital anomalies of the kidney and urinary tract (CAKUT) represent the major cause of chronic renal failure (CRF) in childhood [1]. Recently, we identified the first CAKUT-associated human mutations in the candidate gene *BMP4* (bone morphogenetic protein 4) in a study involving 250 pediatric patients [2]. All five affected patients presented with a spectrum of renal maldevelopment, ranging from kidney agenesis to hypoplasia and dysplasia (with or without cysts). This broad phenotypic spectrum is also observed in mice heterozygous for the knockout of *Bmp4* [3]. In *Gata2* hypomorphic mutant mice, a reduced *Bmp4* abundance results in uropathies also resembling the human CAKUT phenotype [4]. Bmps are a subgroup of the transforming growth factor-beta (TGF-β) superfamily involved in body patterning and the morphogenesis of many organs [5–7]. They also regulate a variety of cellular processes, including differentiation, proliferation, apoptosis, and bone remodeling and repair [8–10]. Ureteric budding (UB) into the metanephric mesenchyme (MM) constitutes a crucial step during early kidney development and is regulated by reciprocal interactions of a complex network of intra- and extracellular signaling proteins and transcription factors [11]. *BMP4* is one of the key regulators in early kidney development. It is strongly expressed in the mesenchymal cells surrounding the Wolffian duct (WD) and is postulated to prevent ectopic budding from the WD or the ureteric stalk. In later stages, it promotes kidney development by stimulating the elongation of the branching ureter within the MM [3]. Bmp4 is synthesized as an inactive 46.5-kDa precursor. The proprotein is then cleaved to yield the active, carboxy-terminal mature protein dimer [12, 13] (Fig. 1). However, the whole molecule is linked noncovalently and is secreted from the cell, similar to the TGF-β molecule [14].

To further elucidate the role of *BMP4* in human kidney development, we performed functional studies with wild-type and mutated forms of Bmp4. All three human missense mutations identified in our CAKUT patients (S91C-, N150K- and T116S-*BMP4*) were analyzed, and we show that mutated Bmp4 behaves differently in biochemical and cellular systems compared with the wild-type protein. These results support our data obtained in zebrafish (*Danio rerio*, a common model organism used for vertebrate genetic research) that human mutations in *BMP4* impair Bmp4 function [2] which, in turn, results in disturbed early kidney development as observed in CAKUT patients.

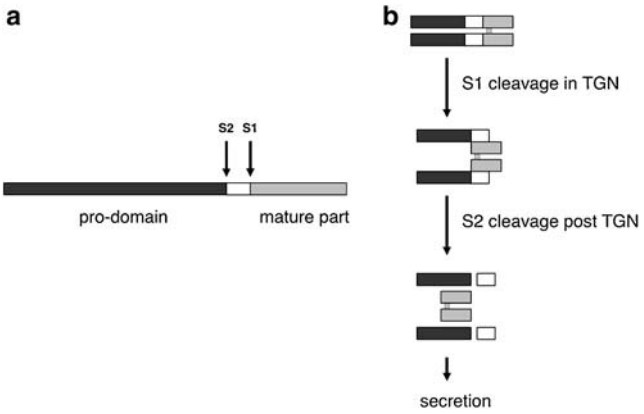

Fig. 1 **a** Bone morphogenic protein 4 (Bmp4) structure, **b** Bmp4 cleavage. *TGN* trans-Golgi network

Methods

In silico analysis of Bmp4 mutants

For the in silico prediction of the pathogenesis of *BMP4* mutations, Web-based software was applied. The PolyPhen program (http://genetics.bwh.harvard.edu/pph/) uses sequence homologies and the mapping of substitution sites to known protein 3D structures [15, 16]. The SIFT program (http://blocks.fhcrc.org/sift/SIFT.html) refers to protein sequence homologies to predict whether an amino acid substitution will affect the function of the protein of interest [17].

Site-directed mutagenesis

A full-length complement DNA (cDNA) (IRAK p961E0727Q) clone of human *BMP4* was obtained from the German Resource Center for Genome Research (RZPD, Berlin, Germany). The entire coding sequence of *BMP4* with exception of the terminal stop codon was subcloned in-frame into a pcDNA3.1/V5-HIS-TOPO vector (Invitrogen, Karlsruhe, Germany). Human *BMP4* mutations were introduced using the QuickChange Site-Directed Mutagenesis Kit (Stratagene, La Jolla, CA, USA). Constructs were rese-

quenced to prove the correct insertion of the human mutations.

Cell culture

COS7 and HEK293 cells were maintained in Dulbecco's modified Eagle's medium (DMEM) (PAA, Coelbe, Germany) supplemented with 10% fetal bovine serum (FBS) (PAA, Coelbe, Germany) at 37°C in a humidified atmosphere of 5% CO_2. Next, 800 µg/ml Geneticin (GIBCO, Invitrogen, Paisley, UK) was added to the culturing medium of stable COS7 cells. For transient transfection of different *BMP4* constructs using FuGENE (Roche, Applied Science, Indianapolis, IN, USA), cells were cultured in antibiotic-free medium.

Real-time RT-PCR

Ribonucleic acid was isolated with the RNeasy Mini Kit (QIAGEN, Hilden, Germany), checked for integrity on an agarose gel, and quantified photometrically. Approximately 1 µg of total RNA (tRNA) was reverse transcribed with oligo (dT)/random hexamer primers (10:1). Real time reverse-transcription polymerase chain reaction (RT-PCR) was performed with the ABI Prism 7000 Real Time PCR system (Applied Biosystems, Foster City, CA, USA) with specific primers for 18 S (forward: 5'-AGTTGGTGGAGC GATTTGTC-3'; reverse: 5'-CGGACATCTAAGGGCAT CAC-3', amplicon length 171 bp), *BMP4* (forward: 5'-AGTGCCGTCATTCCGGACTA-3'; reverse: 5'-GCTCCTCACGGTGTTGGC-3', amplicon 132 bp), and Universal Mastermix (Applied Biosystems) with SYBR green to detect PCR products at the end of each amplification step. Serial dilutions of an arbitrary cDNA pool were used to establish a standard curve. Relative quantities of RNA levels were determined, accounting for amplification efficacy by the software provided with the PCR system. Messenger RNA levels were normalized to corresponding 18-S quantities, determined within the same run. Messenger RNA levels of mutants were then normalized to the mRNA level of the wild type.

Western immunoblotting

Forty-eight hours after transfection or seeding (for stable cells), supernatant was collected and cells were washed once with cold phosphate-buffered saline (PBS) and lysed with ice-cold lysis buffer [20 mM Tris-(hydroxymethyl)-aminomethanhydrochlorid (Tris-HCl), pH 8.0, 150 mM sodium chloride (NaCl), 20 mM sodium fluoride (NaF), 1% Triton X-100, 2 mM ethylenediaminetetraacetic acid (EDTA), 1 mM ethylene glycol tetraacetic acid (EGTA)] containing complete protease inhibitor cocktail (Roche, Mannheim, Germany), vortexed well, and centrifuged for 3 min at 15,500 *g*. The protein content of the supernatant was measured by the Bradford method. The cell supernatant was concentrated using 1.5% deoxycholic acid and 20% trichloroacetic acid (TCA) followed by dissolving the pellet in 0.1 M sodium hydroxide (NaOH). The protein concentration was also measured by the Bradford method. Equal amounts of protein were denatured in 4× sample buffer [0.27 M Tris-HCl, pH 6.8, 11% glycerol, 8.8% sodium dodecyl sulfate (SDS), 0.01% bromphenol blue, with 4% β-mercaptoethanol (ME) or without β-ME for nonreducing analysis], separated by SDS polyacrylamide gel electrophoresis (SDS-PAGE) (7.5–12%) and transferred to Protran nitrocellulose membrane (Whatmann, Dassel, Germany). For analysis of proteins under nonreducing conditions (compared with reducing conditions), SDS-PAGE gels of 7.5% were used. The membranes were blocked in 5% milk and 1% bovine serum albumin (BSA) in Tris buffer containing 0.05% Tween-20 for 1 h at room temperature or overnight at 4°C, then incubated with the indicated antibodies diluted in 5% milk and visualized using chemiluminescent detection system and Hyperfilm ECL films (Amersham Biosciences, Freiburg, Germany) according to the manufacturer's instructions. Equal loading of protein was assessed by reprobing the membrane for β-actin. Primary antibodies were anti-V5 (Invitrogen), 1:30,000 1 h for cell lysate, 1:5,000 O/N for supernatant, anti-Bmp4 (Abcam, Cambridge, MA, USA), 1:500 O/N; anti-β-actin (Abcam), 1:20,000 1 h. Secondary antibody was horseradish peroxidase (HRP) anti-mouse (Cell Signaling, Danvers, MA, USA).

Immunofluorescence

Stably transfected COS7 cells were grown on coverslips. After 48 h, cells were washed and fixed in cold methanol for 10 min at −20°C then permeabilized with 0.3% TritonX-100 for 10 min at room temperature. For V5 staining, cells were washed in PBS, blocked for 30 min at room temperature [PBS, 2% fetal calf serum (FCS), 2% BSA, 0.2% fish gelatin] and incubated with primary antibody (mouse anti-V5, 1:100 in PBS, Invitrogen) overnight at 4°C, washed, incubated with secondary antibody [biotinylated horse anti-mouse immunoglobulin G (IgG), 1:200 in PBS, Vector Laboratories, Burlingame, CA, USA] for 2 h at room temperature, washed again, and then incubated with Cy3-conjugated Streptavidin (1:2,000 in PBS, Jackson ImmunoResearch, West Grove, PA, USA) for 2 h at room temperature. For double staining with lysosome or ER, marker cells were washed again and incubated with second primary antibodies [rabbit anti-lysosomal-associated membrane protein 1 (LAMP1) for lysosomes, 1:100 in PBS, Abcam; rabbit anti-Calnexin for ER, 1:200 in PBS, Abcam] overnight at 4°C. Cells were then

washed and incubated with secondary antibody (Cy2-conjugated AffiniPure goat anti-rabbit IgG, 1:500 in PBS, Jackson ImmunoResearch) for 2 h at room temperature. Nucleos staining was performed with Bisbenzimide H33258 (1:600 in water, stock 1 mg/ml, Serva Electrophoresis, Heidelberg, Germany) for 2 min. Slides were mounted in Mowiol solution and then examined with a Perkin Elmer ERS-FRET spinning disc confocal microscope.

Results

In silico analysis of Bmp4 mutants

In silico analysis of *BMP4* mutations applying the PolyPhen software predicted possibly damaging, benign, and probably damaging for S91C, N150K, and T116S mutants, respectivly. The following predictions were obtained applying SIFT analysis: Substitution at position 91 from S to C and at position 116 from T to S were predicted to "affect protein function", with scores of 0.04 and 0.01, respectively. Substitution at position 150 from N to K was predicted to be "tolerated", with a score of 0.19, indicating a minor effect of N150K on the protein structure of Bmp4 using computational analysis.

Bmp4 mutants have lower mRNA abundance

To test for the functional effect of human mutations in *BMP4* identified in CAKUT patients, we used an overexpression vector with V5 and His epitopes. COS7 and HEK293 cells were transfected with different human *BMP4* constructs expressing wild-type or mutant Bmp4 (S91C, N150K, and T116S). Intense signals observed via Western analysis in cell lysate and supernatant confirmed successful transfection (data not shown). Compared with the wild type, Bmp4 mutants showed a lower levels of mRNA abundance, especially T116S, consistent with the protein levels in the supernatant (Fig. 2), indicating a lower degree of transcriptional efficacy.

S91C mutant Bmp4 forms an extra disulfide bond

Western blot analysis was performed to investigate the protein complexes formed by wild-type and mutant Bmp4 in the presence and absence of reducing agents. Under nonreducing conditions, in the absence of β-ME, the S91C mutant formed an alternative protein complex of approximately 100 kDa (Fig. 3a), whereas adding β-ME as reducing agent resulted in disappearance of this extra band (Fig. 3b). The substitution of Ser91 with a cysteine confers the ability to form abnormal disulfide bonds. To prove this theory, we used dithiothreitol (DTT) as a disulfide bond

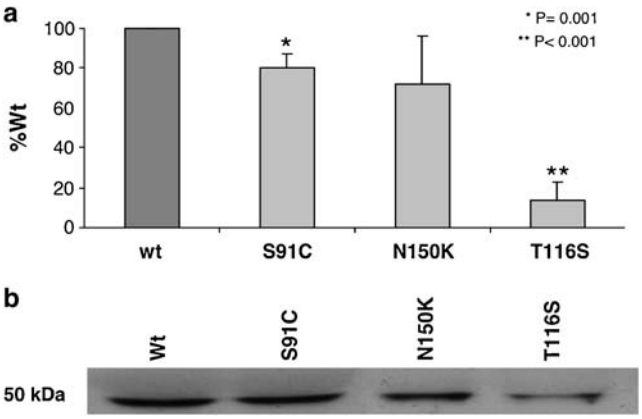

Fig. 2 Bone morphogenic protein-4 (Bmp4) mutants have lower messenger RNA (mRNA) abundance. **a** Real-time quantitative reverse-transcriptase polymerase chain reaction (RT-PCR) assessment of *BMP4* mRNA level in cells transfected with wild-type or mutant construct of *BMP4*. The mRNA levels were first normalized to corresponding 18-S quantities determined within the same run, and then mRNA level of mutants were normalized to that of wild type. **b** Western blot analysis of the supernatant of the transfected cells indicating secreted Bmp4 to culture medium. The same plates were used to harvest cells for Western blot and real-time analysis. Beta-actin controls on the cell lysates (not shown) confirmed comparable protein amounts

blocker and repeated immunoblot analysis with two different antibodies. In the absence of DTT and any other reducing agent, the mutant S91C formed again an alternative protein complex when compared with wild-type Bmp4. Adding DTT caused this complex to disappear (Fig. 4a and b). By applying two different antibodies, we excluded the production of an technical artefact. Moreover, mass spectrometry analysis [matrix-assisted laser desorption/ionization−time of flight (MALDI-TOF)] of purified protein from cells stably expressing Bmp4 confirmed Bmp4 as the protein observed at 50 kDa in nonreducing SDS-PAGE (data not shown).

S91C- and N150K-Bmp4 show perinuclear retention in the ER and lysosomal colocalization

Immunofluorescent staining was performed to determine the intracellular localization of wild-type and mutant Bmp4 in stably transfected COS7 cells. Double staining of Bmp4 and ER demonstrated a partial colocalization for all constructs of Bmp4, as expected for secreted proteins (Fig. 5a). However, a marked perinuclear ER accumulation of Bmp4 was observed for the S91C- and, to a lower degree, for the N150K mutants compared with the wild type, indicating ER retention of S91C- and N150K Bmp4. Subsequent lysosomal staining revealed a higher degree of colocalization of both mutants with cytoplasmic lysosomes, which is in line with enhanced lysosomal degradation of mutated Bmp4 protein (Fig. 5b). No differences were observed between T116S and wild-type Bmp4.

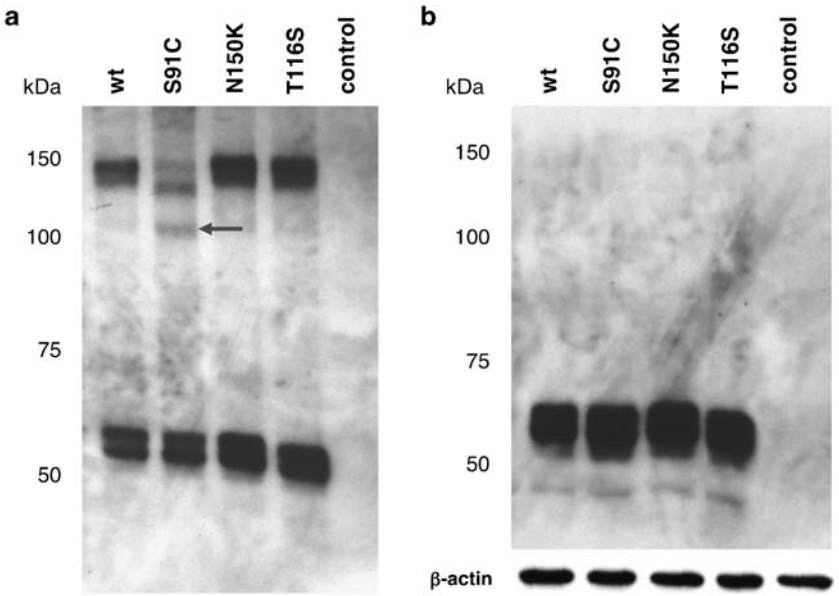

Fig. 3 S91C mutant bone morphogenic protein-4 (Bmp4) forms an alternative protein complex. Western blot analysis with anti-V5-epitope antibody of wild-type and mutant Bmp4 proteins under **a** nonreducing conditions without β-mercaptoethanol, and **b** reducing conditions with β-mercaptoethanol. Equal loading of protein was indicated by detecting of β-actin

Discussion

In this study, three human missense mutations (S91C, N150K, T116S) recently identified in *BMP4* in pediatric CAKUT patients were studied in a cellular expression system. Computational analysis evaluating theoretical effects on protein structure introduced by the above-mentioned mutations revealed significant scores of pathogenicity for S91C and T116S; a minor effect, however, was predicted for N150K. It has been formerly reported that Bmp4 exerts a negative feedback on its own mRNA levels in osteoblast cells. The inhibitory effects of Bmp4 on *BMP4* transcripts are dose dependent and can be transcriptional and posttranscriptional, as has been demonstrated in transcriptionally arrested osteoblast cells [18]. The promotor region of *BMP4* is GC rich with no obvious TATA or CAAT consensus sequences. This region includes positive and negative transcriptional regulatory elements determining the basal expression of *BMP4* [19–21]. However, the exact elements responsible for inhibitory effects of Bmp4 on its transcription have not been defined [19, 20]. The posttranscriptional destabilizing effect of Bmp4 on its mRNA could contribute to auto-downregulation of *BMP4* expression. Although the exact mechanisms involved in posttranscriptional control of *BMP4* expression have not been yet elucidated, regulation of cytosolic proteins binding to the 3′ untranslated region or to other regions of the *BMP4* RNA could be taken into consideration as a probable

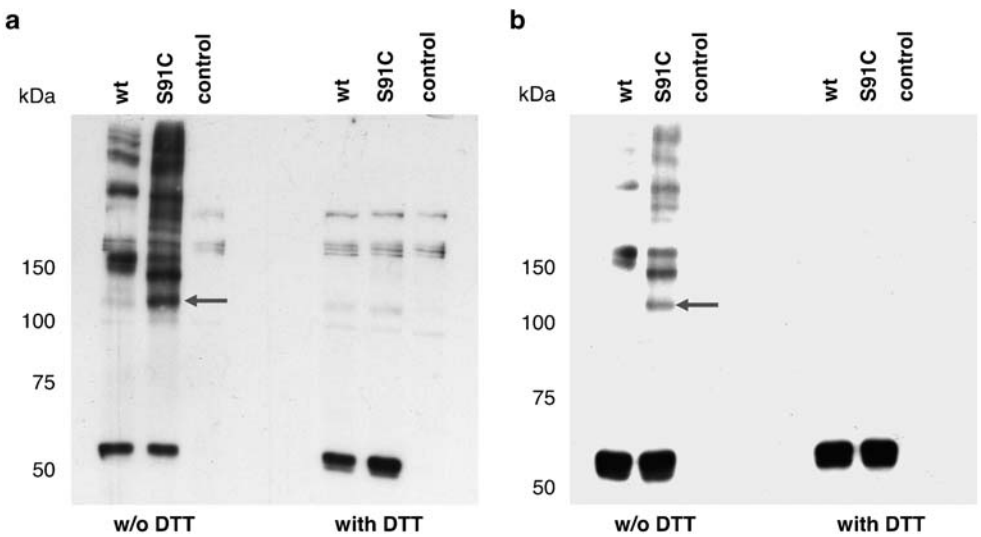

Fig. 4 S91C mutant bone morphogenic protein-4 (Bmp4) forms an extra-disulfide bond. Western blot analysis of wild-type and mutant Bmp4 proteins in the absence of β-mercaptoethanol with or without disulfide bond blocker dithiothreitol (DTT). Detection with **a** anti-Bmp4 Ab and **b** anti-V5 Ab

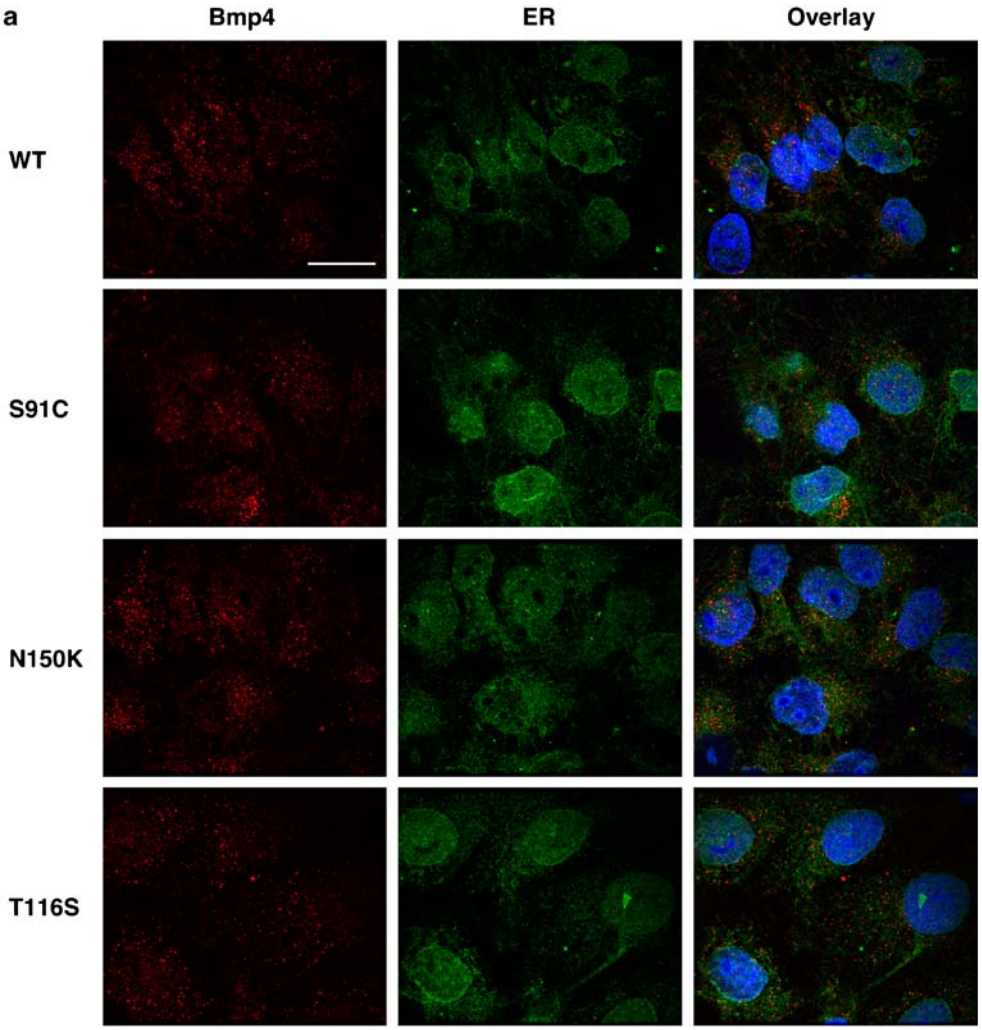

Fig. 5 S91C and N150K bone morphological protein-4 (Bmp4) mutants show alterations of subcellular localization. **a** Double staining of Bmp4 and endoplasmic reticulum (ER). S91C and N150K mutants showed perinuclear accumulation of signals. **b** Bmp4 and lysosome double staining revealed that S91C and N150K mutant Bmp4 colocalize with lysosomes. *White scale bar* indicates 20 μm

mechanism [22, 23]. The lower levels of mRNA abundance of mutant *BMP4* observed in this study indicate a lower degree of transcriptional efficacy and suggest stronger inhibitory effects of mutant Bmp4 on its RNA. This effect was most profound for the T116S-mutant.

Bmp4 is a member of TGF-β superfamily and secreted probably as part of a latent complex into the extracellular matrix. Mature Bmp4 is proteolytically separated from the pro domain, but both fragments remain noncovalently linked. All three missense mutations identified in *BMP4* locate to the pro domain of the protein. Interestingly, it has recently been demonstrated for *BMP15* that a human pro domain mutation causes ovary dysgenesis, and Western blot analysis of the mutant Bmp15 revealed alterations of protein assembly due to formation of an extra disulfide bond [24]. We have now identified a similar effect for the S91C-Bmp4 mutant in this study and confirmed in a cellular expression system that S91C-Bmp4 forms an additional disulfide bond associated with abnormal protein folding, a probable precursor−mature protein dimer. This abnormal protein dimer could impair pro-protein processing, which results in possible alterations of the production of bioactive peptides. Furthermore, secretion of unprocessed or misprocessed protein products will also affect the interaction of *BMP4* with its target receptors.

Folding of secreted proteins takes place in the ER after translocation from the cytoplasm in an unfolded state; here, they are modified and folded to acquire their biologically active conformation [25]. In fact, the ER is part of the cell quality control machinery to discriminate between properly folded proteins and terminally misfolded species, as well as unassembled protein subunits [26]. Misfolded proteins are subjected to degradation after this proof-reading procedure [27]. However, the ER is not the only quality control checkpoint of the cell. Some mutant proteins with minor conformational defects pass the ER but are subsequently detected as abnormal or misfolded and targeted to lysosomes for degradation [28], among them, mutated proteins with only one amino acid exchange [29]. In this study, we provide evidence that S91C-Bmp4 and—

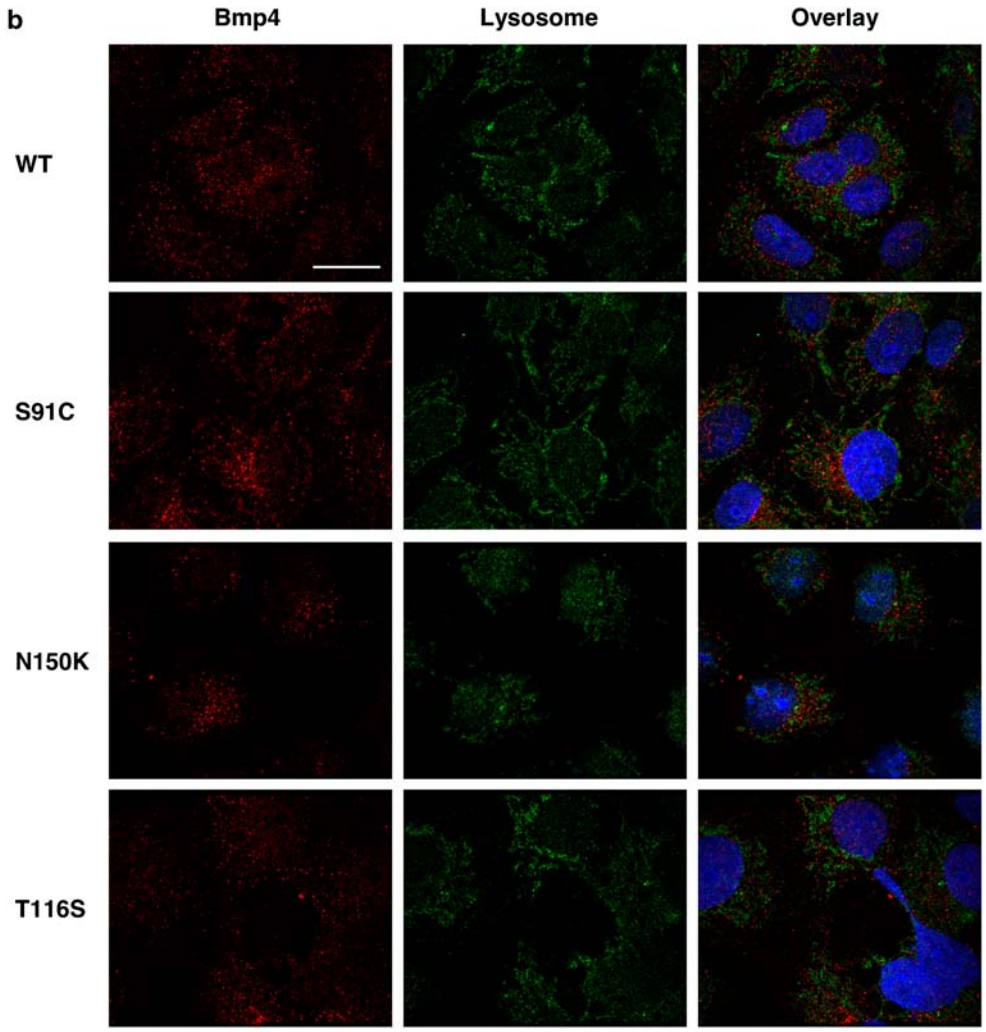

Fig. 5 (continued)

to a lower degree—N150K-Bmp4 accumulate in the perinuclear ER. Lysosomal staining revealed enhanced lysosomal degradation of mutated Bmp4 protein. Alterations of protein complex formation and protein misfolding seem to be one aspect of Bmp4 dysfunction, especially of the S91C mutant.

More recently, the S91C-mutation in *BMP4* has also been reported in a patient with subepithelial cleft lip [orbicularis oris muscle (OOM) defect] [30]. In that study, 1,085 DNA samples of patients with subepithelial, microform, or overt cleft lip were sequenced in *BMP4*, and interestingly, mutations were identified in eight affected individuals (and excluded in 529 controls), among these, one patient with the S91C-*BMP4* mutation. The phenotype in this patient was subclinical, detectable only by ultrasound. No data concerning malformations of other organ systems in carriers of *BMP4* mutations was available in that study. It therefore remains speculative whether a subset of these individuals is also affected by a CAKUT phenotype. As Bmp4 is involved in the pathogenesis of many organs, especially of muscle, bone, and brain, extrarenal phenotypes may be adequately explained. Very recently, another report appeared for publication describing pathogenic mutations in *BMP4* in a subset of patients with eye, brain, and digit developmental anomalies [31]. These patients present with anophthalmia-microphthalmia (AM), brain malformations, and polydactyly. One patient was also affected by cryptorchidism; however, no other kidney or urinary tract anomalies were reported in the patient cohort. Most probably, this overall phenotypic variation observed in *BMP4* mutation carriers is due to major differences in the genetic backgrounds of affected individuals. The intraindividual accumulation of sequence variations in different developmental genes might be one aspect of differing genetic backgrounds on which the mutations in *BMP4* appeared. Following this

idea, the organ manifestation might be dependent on the expression patterns of the most dominant genes involved (dominant either in number or in function). Alternatively, or in addition, nongenetic endogenous or environmental factors might also play a role. Large collaborative studies involving different clinical subspecialties will be required to more precisely define genotype–phenotype correlations in all carriers of *BMP4* mutations identified so far.

Acknowledgement The authors acknowledge the Nikon Imaging Center at the University of Heidelberg. Financial support for this study was obtained from the Thyssen Foundation (AZ-10.07.2.173), the Dietmar Hopp Foundation, and the European Commission (5th Framework Program, QLG1-CT-2002 00908).

References

1. Woolf AS (2000) A molecular and genetic view of human renal and urinary tract malformations. Kidney Int 58:500–512
2. Weber S, Taylor JC, Winyard P, Baker KF, Sullivan-Brown J, Schild R, Knüppel T, Zurowska AM, Caldas-Alfonso A, Litwin M, Emre S, Ghiggeri GM, Bakkaloglu A, Mehls O, Antignac C, Network E, Schaefer F, Burdine RD (2008) *SIX2* and *BMP4* mutations associate with anomalous kidney development. J Am Soc Nephrol 19:891–903
3. Miyazaki Y, Oshima K, Fogo A, Hogan BL, Ichikawa I (2000) Bone morphogenetic protein 4 regulates the budding site and elongation of the mouse ureter. J Clin Invest 105:863–873
4. Hoshino T, Shimizu R, Ohmori S, Nagano M, Pan X, Ohneda O, Khandekar M, Yamamoto M, Lim KC, Engel JD (2008) Reduced BMP4 abundance in Gata2 hypomorphic mutant mice result in uropathies resembling human CAKUT. Genes Cells 13:159–170
5. Hogan BL (1996) Bone morphogenetic proteins: multifunctional regulators of vertebrate development. Genes Dev 10:1580–1594
6. Hogan BL (1996) Bone morphogenetic proteins in development. Curr Opin Genet Dev 6:432–438
7. Ducy P, Karsenty G (2000) The family of bone morphogenetic proteins. Kidney Int 57:2207–2214
8. Dale L, Jones M (1999) BMP signaling in early Xenopus development. BioEssays 21:751–760
9. Shum L, Nuckolls G (2002) The life cycle of chondrocytes in the developing skeleton. Arthritis Res 4:94–106
10. von Bubnoff A, Cho KW (2001) Intracellular BMP signaling regulation in vertebrates: pathway or network? Dev Biol 239:1–14
11. Piscione TD, Rosenblum ND (2002) The molecular control of renal branching morphogenesis: current knowledge and emerging insights. Differentiation 70:227–246
12. Cui Y, Hackenmiller R, Berg L, Jean F, Nakayama T, Thomas G, Christian JL (2001) The activity and signaling range of mature BMP-4 is regulated by sequential cleavage at two sites within the prodomain of the precursor. Genes Dev 15:2797–2802
13. Degnin C, Jean F, Thomas G, Christian JL (2004) Cleavage within the prodomain direct intracellular trafficking and degradation of mature bone morphogenetic protein-4. Mol Biol Cell 15:5012–5020
14. Annes AP, Munger JS, Rifkin DB (2003) Making sense of latent TGFβ activation. J Cell Sci 116:217–224
15. Sunyaev S, Ramensky V, Koch I, Lathe W 3 rd, Kondrashov AS, Bork P (2001) Prediction of deleterious human alleles. Hum Mol Genet 10:591–597
16. Ramensky V, Bork P, Sunyaev S (2002) Human non-synonymous SNPs: server and survey. Nucleic Acids Res 30:3894–3900
17. Ng PC, Henikoff S (2003) SIFT: predicting amino acid changes that affect protein function. Nucleic Acids Res 31:3812–3814
18. Pereira RC, Rydziel S, Canalis E (2000) Bone morphogenetic protein-4 regulates its own expression in cultured osteoblast. J Cell Physiol 182:239–246
19. Feng JQ, Chen D, Cooney AJ, Tsai MJ, Harris MA, Tsai SY, Feng M, Mundy GR, Harris SE (1995) The mouse bone morphogenetic protein-4 gene. J Biol Chem 270:28364–28373
20. Ebera S, Kawasaki S, Nakamura I, Tsutsumimoto T, Nakayama K, Nikaido T, Takaoka K (1997) Transcriptional regulation of the mBMP-4 gene through an E-box in the 5′-flanking promotor region involving USF. Biochem Biophys Res Commun 240:136–141
21. Shore EM, Xu M-Q, Shah PB, Janoff HB, Hahn GV, Deardorff MA, Sovinsky L, Apinner NB, Zasloff MA, Wozney JM, Kaplan FS (1998) The human bone morphogenetic protein 4 (BMP-4) gene: molecular structure and transcriptional regulation. Calcif Tissue Int 63:221–229
22. Greenberg ME, Belasco JG (1993) Control of decay of labile protooncogene and cytokine mRNAs. In: Belasco J, Brawerman G (eds) Control of messenger RNA stability. Academic Press, New York, pp 199–215
23. Delany AM, Canalis E (1998) Basic fibroblast growth factor destabilizes osteonectin mRNA in osteoblasts. Am J Physiol 274: C734–740
24. Di Pasquale E, Beck-Peccoz P, Persani L (2004) Hypergonadotropic ovarian failure associated with an inherited mutation of human bone morphogenetic protein-15 (Bmp15) gene. Am J Hum Genet 75:106–111
25. Haigh NG, Johnson AE (2002) Protein sorting at the membrane of the endoplasmic reticulum. In: Dalbey RE, von Heijine G (eds) Protein targeting, transport and translocation. Academic Press, London, pp 74–106
26. Ellgaard L, Molinari M, Helenius A (1999) Setting the standards: quality control in the secretory pathway. Science 286:1882–1888
27. Kostova Z, Wolf DH (2003) From whom the bell tolls: protein quality control of the endoplasmic reticulum and the ubiquitin-proteasome connection. EMBO J 22:2309–2317
28. Trombetta ES, Parodi AJ (2003) Quality control and protein folding in the secretory pathway. Annu Rev Cell Dev Biol 19:649–676
29. Buscà R, Martinez M, Vilella E, Pognonec P, Deeb S, Auwerx J, Reina M, Vilaro S (1996) The mutation Gly142Glu in human lipoprotein lipase produces a missorted protein that is diverted to lysosomes. J Biol Chem 271:2139–2146
30. Suzuki S, Marazita ML, Cooper ME, Miwa N, Hing A, Jugessur A, Natsume N, Shimozato K, Ohbayashi N, Suzuki Y, Niimi T, Minami K, Yamamoto M, Altannamar TJ, Erkhembaatar T, Furukawa H, Daack-Hirsch S, L'heureux J, Brandon CA, Weinberg SM, Neiswanger K, Deleyiannis FW, de Salamanca JE, Vieira AR, Lidral AC, Martin JF, Murray JC (2009) Mutation in BMP4 are associated with subepithelial, microform and overt cleft lip. Am J Hum Genet 84:406–411
31. Bakrania P, Efthymiou M, Klein JC, Salt A, Bunyan DJ, Wyatt A, Ponting CP, Martin A, Williams S, Lindley V, Gilmore J, Restori J, Robson AG, Neveu MM, Holder GE, Collin JR, Robinson DO, Farndon P, Johansen-Berg H, Gerrelli D, Ragge NK (2008) Mutation in *BMP4* cause eye, brain and digit developmental anomalies: overlap between the *BMP4* and hedgehog signaling pathways. Am J Hum Genet 82:304–3192